INTERNATIONAL CONFERENCE OF AGRICULTURAL ECONO
IGAE
29th | Milan Italy 2015
UNIVERSITÀ DEGLI STUDI DI MILANO AUGUST 8 - 14
AGRICULTURE IN AN INTERCONNECTED WORLD

Process-based simulation of regional agricultural supply functions in Southwestern Germany using farm-level and agent-based models

By Christian Troost and Thomas Berger,

Land Use Economics in the Topics and Subtropics,
Universität Hohenheim, Germany

In combination with crop growth models, farm-level models allow an in-depth, process-based analysis of farmer adaptation to climate change and agricultural policy. Evaluated for all farms in an area and extended by interactions, farm-level models become agent-based models that allow simulating aggregate regional production and structural change. Confined to a local or regional scope, however, they cannot directly incorporate price feedbacks that play out at global scale. In this contribution, we use experimental designs to evaluate a non-connected agent-based model for the full space of potential future price developments. We discuss and compare the use of standard regression analysis and non-parametric, automatic methods (MARS and Kriging) to summarize supply behavior over the simulated price ranges. Estimated supply functions constitute a surrogate model for the original agent-based model and could be used to iterate detailed regional analysis with national or global market models in an efficient way.

IAAE

1. Introduction

Climate change has the potential to profoundly affect agriculture in many regions of the world and confront farmers with conditions that have not been observed in their area before. Given this potential for structural shifts in agricultural production systems, scientists cannot simply rely on statistical analysis of past observations to extrapolate future agricultural supply and policy response (Antle and Capalbo 2001). Mathematical programming farm- and household-level models (both, farm-level MP models and agent-based models) can play a key role in analyzing the consequences of climate change for agricultural production and livelihoods (van Wijk et al. 2012): Combined with crop growth models, they are arguably the closest equivalent to process-based models available to agricultural economists. They are able to reflect the complex interlinkages between different production options, farm resources, farmer characteristics, and household objectives and provide the necessary whole-farm perspective needed for adaptation analysis (Reidsma et al. 2010). They are able to incorporate projected, but unobserved changes in yield responses, but also climate impacts not reflected in yield simulations (Troost and Berger 2015). If run for all (or a sufficiently large and representative set of) farms of an area, they can capture the regional heterogeneity of vulnerability and adaptative capacity and enhanced with interactions they become agent-based models that help to analyse innovation diffusion, cooperation, local resource conflicts and local, fragmented market outcomes (Berger and Troost 2014). In short, they provide the means to base *ex ante*, out-of-sample analysis on a combination of theoretical and empirical process knowledge.

However, the greatest strength of farm-level models is also their most important weakness: the ability to model real-world processes explicitly and to reflect heterogeneity and locally specific conditions requires very detailed data and knowledge of the agricultural system under study (Buysse et al. 2007). Their scope is therefore usually confined to local or regional scales and it is not always easy to upscale these models or generalize results (Gibbons et al. 2010).

This regional confinedness also means that feedbacks with global or national agricultural markets cannot be simulated directly, so that the model remains ignorant to price changes

triggered by the simulated climate adaptation response. Moreover, it may be anticipated that climate change effects may differ with the prevailing agricultural crop prices. For this reason, a meaningful simulation analysis has to evaluate climate change effects over the full range of anticipated future price developments. Depending on the computational complexity of the model, this can be challenging. Still, if the farm-level model is run for a sufficiently large share of farms in the area, such an analysis cannot only highlight the price level dependency of climate change impacts, but will provide a process-based estimate of potential shifts in regional crop supply functions caused by climate change.

In this contribution, we demonstrate the use of a non-connected agent-based model, a farm-level model that is solved for every (full-time) farm in the Central Swabian Jura (Southwest Germany), for a process-based, bottom-up simulation of climate change effects on agricultural supply functions. After presenting the study area and model in the next section, Section 3 explains the experimental design we used to cope with the uncertainty and considerable run-time of the model. Section 4 analyzes the simulated dependency of agricultural supply on prices and model uncertainty, and shifts in supply caused by three climate adaptation scenarios. Section 5 discusses outcomes and the merits of different statistical methods used for summarizing supply functions. Section 6 concludes.

2. The Farm-level Model for the Central Swabian Jura

2.1. Study Area

The Central Swabian Jura is a low mountainous area (650-850 m.a.s.l.) that covers about 1,300 km² and located between Stuttgart and Ulm in Southwest Germany. Agriculture in this area is characterized by a relatively balanced mix of crop production, dairy farming, bull fattening, pig production, and biogas production. Most farm holdings simultaneously produce three to five different crops, with summer barley, winter wheat, winter barley and winter rapeseed being the dominant crops, while dairy and cattle farmers tend to also grow silage maize, clover and field grass. Farmer production decisions have to respect a complex set of crop rotation constraints, feed and manure balances, machinery and labor capacity constraints, and policy restrictions.

The area has mostly shallow soils and a comparatively harsh climate (mean annual temperatures around 7 °C, mean annual precipitation 800-1,000 mm) that has been a constraining factor for agricultural production when compared to neighboring regions. Besides producing changes in expected crop yields, climate change might relax current weather constraints on field work: Field work requires suitable weather conditions and farmers need to plan production such that they can muster the necessary amount of labor and machinery power with sufficient certainty within a critical time-slot. In a warmer climate, these windows of opportunity may widen. This would also relax crop rotation constraints: Currently, late wheat harvest dates that overlap with rapeseed sowing dates make wheat-rapeseed sequences infeasible for most farms in the study area. If wheat could be harvested slightly earlier or rapeseed sown slightly later, this might become an important crop rotation option (Troost and Berger 2015).

2.2. The Model

Our analysis builds on the farm-level model that was originally developed in Troost et al. 2012 and Troost and Berger 2015. It consists of a mixed integer programming (MIP) model representing the generic production and investment problem of farmers on the Central Swabian Jura. This MIP problem is solved for each full-time farm in the area setting capacities (and a few farm-specific matrix coefficients) according to the observed characteristics of the farm. The complete MIP matrix comprises around 6,900 variables in about 3,800 equations. In the following, we will summarize only the main features of the model. A full documentation of the MPMAS Central Swabian Jura model including all equations can be found in in the electronic supplement to Troost & Berger 2015 or in Troost 2014.

The model has been implemented using the agent-based software package MPMAS (Schreinemachers & Berger 2011), although the model as used in the present article does not include any agent-agent interactions (i. e. it is a non-connected agent-based model in the definition of Berger et al. 2006). Still, in keeping with MPMAS conventions, we will use the term farm agent to refer to the model representation of an individual farm throughout this article.

Solving the MIP, each farm agent allocates production factors (land, labor and capital) such that they maximize expected farm income given its individually specific resources and production

options, sales and input prices, and the technical and agronomic constraints governing agricultural production. Expected farm income is the sum of revenues from crop production (R_c), animal husbandry (R_h), biogas production (R_b) and received premiums from EU CAP and MEKA schemes (R_p) subtracting variable costs (V), fixed costs (respectively annualized investment cost for new investments) (F), and the balance of interest paid and received (I) as shown in Equation 1. Here $\mathbf{p}_e$ denotes expected prices; $\mathbf{y}_e$, expected yields; **a,** crop and grassland activities; **f,** the part of the crop that is used as animal feed; **h**, animal husbandry activities; **k,** biogas production; z, the first year of biogas production; **M**, machinery owned and employed; **B**, buildings and infrastructure owned; $\mathbf{A}_r$, the amount of land rented in and l, hired labor.

$$max!\,\pi_e = R_c(\boldsymbol{p_e}, \boldsymbol{y_e}, \boldsymbol{a}, \boldsymbol{f}) + R_h(\boldsymbol{p_e}, \boldsymbol{h}) + R_b(\boldsymbol{k}, z) + R_p(\boldsymbol{a}, \boldsymbol{h}) - V(\boldsymbol{p_e}, \boldsymbol{a}, \boldsymbol{h}, \boldsymbol{f}, \boldsymbol{M}, l) - F(\boldsymbol{p_e}, \boldsymbol{B}, \boldsymbol{M}, \boldsymbol{A_r}) + I$$

(Eq. 1)

The model as used in the present article allows for investments in farm machinery and biogas plants. Crop production comprises winter wheat, winter rapeseed, summer malting barley, summer and winter fodder barley, silage maize, field grass production and fallow on arable land as well as grassland cultivation at four levels of intensity (abandonment, extensive use, 2 or 3 uses per year) and with five potential uses: hay, grass silage, pasture, cutting of fresh grass for direct feeding as well as late and very late maintenance cuts compatible with MEKA requirements. The agents distinguish nine different soil classes for arable land, which affect crop yields and tractor power required for field work. Crop yields are based on simulations with the crop modeling package Expert-N using the parameterization developed by Aurbacher et al. (2013). Grassland is considered a separate soil class, which has not been subdivided further. Grass yields depend only on management and are based on grass regrowth functions calculated from data by Berendonk (2011). Crop production is constrained by the field work capacity of the farm, which is calculated as a function of labor and machinery endowments as well as expected days with suitable weather.[1] Also, agronomic limits to crop shares in the rotation and preceding-following crop relationships have to be respected. Possible preceding-following crop relationships are shown in Table 1. It is important to notice that under current climate conditions

1 For a detailed discussion, cf. Troost and Berger 2015.

farmers are virtually forced to grow either summer barley or fallow between wheat and winter rapeseed.

Animal production comprises dairy production, calf and heifer raising, bull fattening, suckler cow herding, piglet production and raising, and pig fattening and is constrained by existing stable capacities and the manure usage of crop production. Animal feeding requirements have been formulated in terms of nutrient and fiber demands (LfL 2010, 2011) allowing the farm agent a great deal of flexibility in the combination of bought and self-produced fodder. Other inputs and labor demands are based on extension service data (KTBL 2010). Sales, input and machinery prices are based on public statistical and extension service data (destatis 2012d; KTBL 2011; LEL 2010, 2011a,b).

For their model, Troost and Berger (2015) created a sample of agent populations, each of which contains one model agent for each full-time farm in the area. Due to privacy restrictions, a direct reproduction of observed farms was not possible. Instead, they used a sampling and matching algorithm to create synthetic, but statistically consistent agent populations for the study area combining information from Agricultural Census and Farm Structure Survey data (FDZ 2010), a farm survey as well as population statistics (destatis 2011, 2012a-c). For each of the years 1999, 2003, and 2007, several agent populations were created. The simulations in this article use the sample of agent populations representing the 533 full-time farm households observed in 2007.

3. Scenarios and Experimental Design

3.1 Price Variation

To be able to estimate supply functions, we need to evaluate the model over the full range of potential price combinations. The time-series of prices observed between 2000-2009 serves as the basis to determine price ranges for crops, animal products and important inputs that were then expressed as coefficients (pc_x) relative to the 2000-2009 price average($\bar{P}_x$).[2] To take account of the fact that crop prices are correlated and usually move in similar directions, price

2 For the simulations, we then extended the ranges by about 20-30% at both ends, to capture also unobserved but not unrealistic price relations.

coefficients (prw_x)for grain maize, malting and fodder barley, rapeseed and animal feed (ready-mixes, soy and rapeseed meal, etc.) were expressed relative to the development of the wheat price, which consequently served as general crop price level. As an example, the price coefficient of malting barley was calculated as $prw_{mb} = \frac{P_{mb,t}}{\bar{P}_{mb}} * pc_{wh,t}$ and the malting barley price in the simulations was consequently calculated as $P'_{mb} = \bar{P}_{mb} * pc_{wh} * prw_{mb}$. It is important to notice that prw_{mb} is not the malting barley to wheat price ratio, but its relative change compared to the 2000-2009 average. The new price ratio can be determined by multiplying prw_{mb} with the original price ratio $\frac{\bar{P}_{mb}}{\bar{P}_{wh}}$. The 11 price coefficients used and their ranges are shown in Table 2.

3.2 Scenarios

To illustrate how supply functions might change in response to climate change and agricultural policy, we repeat the simulation experiment for three different scenarios defined in Troost and Berger (2015): Baseline scenario `B', is based on the crop yields simulated for 1981-2010 weather observations, the current distribution of days suitable for field work and no rapeseed-after-wheat rotations. The climate adaptation scenario C1 reflects a 'standard' assessment that considers only yield effects. It is based on yields simulated for the 2000-2030 WETTREG projection retaining current rotation options and field work days. The extended adaptation scenario C2, on top of yield changes, also considers the additional climate impacts explained in Section 2.1: Wheat-rapeseed rotations become possible and weather constraints on field work are relaxed to become similar to current conditions in neighboring lower-lying regions.

3.3 Model Uncertainty

Farm-level models that are based on theoretical and empirical process knowledge are typically subject to considerable uncertainty as the necessary data is not available in the required depth and breadth for a full region (Buysse et al. 2007). Standard technical coefficients have to be used, parameters have to be chosen ad hoc, parameter variability has to be neglected, processes are omitted and other process representations are uncertain or incomplete. Good modeling practice

requires to clearly communicate this uncertainty to readers and analyze it in order to assess the robustness of results and, on the long run, improve process understanding (Jakeman et al. 2006). One should therefore refrain from identifying a single parameter combination that best fits observation data. For the Central Swabian Jura model, for example, Troost and Berger reduced the parameter space only, where clearly superior settings could be determined in a conservative calibration experiment that tested parameter combinations against three structurally different observation years and then used an elementary effects screening 8Campolongo et al. 2007) to determine the 11 of the 19 unfixed parameters that caused the greatest variance in simulated differences between their climate and price scenarios (cf. Table 3) (Troost and Berger 2015). As a consequence, the Central Swabian Jura model has to be solved repeatedly to cover the space spanned by these 11 parameters and model results are communicated as ranges over this parameter space.

3.4 Experimental Design

For the present analysis, we extend the experimental design of Troost & Berger in order to allow for the estimation of crop supply functions. With a model runtime of about 20-30 minutes for a single period, it is infeasible to evaluate the model for all the potential value combinations – or a full factorial design – of 11 price coefficients, 11 uncertain parameters and 3 scenarios. In such a situation, Latin hypercube sampling(McKay et al. 1979) allows the fullest coverage of a parameter space when the number of model runs is limited. For our simulation experiments, we created a Latin Hypercube design with 600 design points covering the combination of the 11 price coefficients and the 11 parameters. The full sample is evaluated for each of the 3 scenarios. As common in the sensitivity analysis literature (Saltelli et al. 2004), we will use the term input factors when we refer to these 22 parameters from which the LHS is formed.

4. Analyzing Simulated Climate Change Effects on Supply Functions

To provide an illustrative example, we will concentrate our result analysis on changes in market transactions of wheat and barley under potential climate change conditions. As we will see, these two crops are especially suited to highlight the complexity and mutual interdependence of production and supply responses of different crops in the study area. As mentioned above, the

model distinguishes winter fodder barley, summer fodder barley and malting barley production, where the later is exclusively cultivated as a summer crop. Malting barley also is a pure cash crop, while fodder barley and wheat can be sold, but also used for animal feeding. Some of the farmers in the model are net buyers of wheat or fodder barley making also the demand for these crops an interesting output of the model.

4.1 Means and Variation of Climate Change Effects

It is important to understand that by repeating each design point of the LHS for each of the three scenarios, we can control for model uncertainty and price variation and isolate the pure effect of the adaptation scenarios. A first overview of climate change effects on barley and wheat market transactions is show in Table 4. The first column shows the relative standard deviation (= the absolute value of the coefficient of variation) of the supply response in the baseline with respect to the design points of the LHS. It provides an indication in how far the supply or demand for the crop is affected by price variation and model uncertainty. The second and fourth columns, show the mean difference between the baseline and the adaptation scenarios over all design points normalized by the mean supply observed (Md1/Mb, Md1/Mb). It provides a measure for the average effect of the respective climate adaptation scenario. The third and fifth columns show the relative standard deviation of this scenario effect indicating how strongly it varies over the design points of the LHS.

In the climate scenarios, we observe a strong increase in wheat sales and comparable reduction in fodder barley sales, wheat purchases are also strongly reduced, while fodder barley purchases increase slightly on average. In all four cases, the effect of the additional impacts in scenario C2 is to exacerbate the yield effect isolated in C1. In the case of malting barley sales, this is different. Malting barley shows a considerable supply increase on average for C1 with non negligible variation over the LHS design points. In C2, by contrast, the average effect is close to zero, still the high relative variance over the LHS shows that it differs strongly with price effects (in this case that it is positive in some and negative in other cases). This could mean that the climate change effect shifts or turns the supply function or that the climate change effect is affected by the uncertainty in the model.

4.2 Distance Correlations

As a first step towards disentangling the influence of price variation and model uncertainty on supply, Table 5 shows the correlation of the outcome variables with selected price coefficients and model parameters in the LHS. In order to capture also non-linear and non-monotonous correlations, we chose to calculate distance correlations (Szekely et al. 2007; Szekely and Rizzo 2013; Rizzo and Szekely 2013) instead of the common Pearson's correlation coefficient or Spearman's rank correlation. The distance correlation coefficient ranges between 0 (independence) and 1 (perfect correlation). As a consequence of capturing also non-monotonous relationships, they cannot indicate the sign of the correlation. For comparison, the distance correlation between the input factors in the LHS did not surpass 0.1 for any pair of parameters underlining that the sample was largely uncorrelated as desired.

As we can see from the table, the malting barley supply is, as one might expect, correlated with the price coefficients for malting barley, wheat and fodder barley. There is no correlation with any of the uncertain model parameters that would be worth mentioning. (The table includes only those input factors that show a distance correlation greater than 0.1 with any of the five outcome variables.) While this does not completely rule out higher-order influences of model uncertainty, it strongly suggests that the observed variance in climate change effects is not caused by model uncertainty. Between the scenarios we only observe minor changes in correlations. In contrast to malting barley supply, wheat supply is correlated with all crop price coefficients and several model parameters. Here, we can also observe a major change in correlations between scenarios: From B over C1 to C2, the correlation of wheat sales with the relative malting barley price coefficient – which we have to interpret as the influence of the malting barley-to-wheat price ratio on wheat sales in our modeling context – increases, while the correlation with the relative fodder barley price coefficient decreases. At the same time, the correlation between wheat and malting barley sales (not shown in the table) increases from 0.11 in scenario B to 0.46 in C2, while the correlation of wheat and fodder barley sales decreases from 0.41 to 0.26.

4.3 Scatter Plots and LOWESS Smoothing

As often in any data analysis, it is a good idea to use scatter plots to get a first impression of the relationship between the outcome of interest and its major determinants. Figure 1 shows a scatter plot of the simulated malting barley (a) and winter wheat (b) production quantities. Each dot represents one of the design points of the LHS600 sample. Dots are ordered along the x-axis according to the malting barley-to-wheat price ratio assumed for that design point. Red dots represent the design points of the baseline scenario B, yellow and blue dots represent adaptation scenarios C1 and C2, respectively. The variance in simulated production quantities for similar malting barley-to-wheat price ratios is caused by the differing assumptions for the other input factors at each design point.

For each scenario, we overlaid a nonparametric LOWESS smoother to highlight the median response of malting barley and wheat production to the malting barley-to-wheat price ratio. As expected, malting barley production increases with an increasing ratio in all scenarios. In scenarios B and C1, the variance around the smoothing line is considerably higher at ratios between 1 and 1.3 than at higher or lower values. This phenomenon can be explained by the specific constraints to crop rotation in the area: At current climate conditions, most farmers are virtually forced to grow summer barley at some point in their crop rotation. At lower malting barley-to-wheat price ratios, the reduction in malting barley area is compensated by an increase in summer fodder barley as shown in Figure 1 (c) leading to a near-flattening of the response curve of the summer barley area at lower price ratios (Fig. 1 d). The exact point at which farmers switch from malting to summer fodder barley is, of course, mainly determined by the malting barley-to-fodder barley price ratio (Fig. 1 e). This explains the correlation of malting barley production to the fodder barley-to-wheat price ratio we observed in the previous section.

The adaptation scenario C1 assumes an increase in wheat yields, an increase in summer barley yields on some soils and a decline in winter barley yields (Figs. 1 a,b). As a consequence, the simulation results show an increase in both, winter wheat and summer barley production compared with the baseline scenario. This production increase is a consequence of both the higher yields and an increase in the area allocated to these crops. Adaptation scenario C2 allows the additional rotation option winter rapeseed after winter wheat eliminating the need to grow

summer barley for rotational reasons for many farmers. This leads to a general increase of winter wheat production at the cost of both, summer fodder and malting barley production, except at high malting barley-to-wheat price ratios. As a consequence, at ratios between 1.2 and 1.4, both, malting barley and wheat production are much more sensitive to price relation changes in scenario C2 than in the baseline or scenario C1.

Since a reduction of malting barley area is compensated by an increase in summer fodder barley in B and C1, changes in the malting barley-to-wheat price ratio indirectly affect the fodder barley market. As we can see from Figure 2, the additional fodder barley production is mainly absorbed by increased fodder barley sales (a), while the amount of fodder barley used for feeding (b), winter fodder barley production (c), and fodder barley purchases (d) remain more or less unaffected by the malting barley-to-wheat price ratio. Both, adaptation scenarios lead to a reduction in winter barley production, which is uniform along the malting barley-to-wheat price ratio, though it is stronger in C2 than in C1. In scenario C1, this reduction is partly compensated by increased summer fodder barley production at low malting barley-to-wheat price ratios. As purchased and used amounts of fodder barley remain, again, largely unaffected, scenario C1 leads to a steeper, more sensitive price response curve of fodder barley supply, while scenario C2 shows merely a shift of the price response curve to lower levels.

4.4 Regression Models

With that in mind, we can now e. g. estimate a regression model for malting barley supply in the study area based on our simulation results. Given our analysis in the previous section, we formulate the following regression model for malting barley supply:

$$q_{mb,s} = \beta_0 + \beta_1 D + \beta_2 D P_{m/w} + \beta_3 D P_{m/f} + \beta_4 D P_w \qquad \text{(Eq. 2)}$$

where D is a dummy variable that is 1 if the malting barley-to-fodder barley price ratio is greater than 1.1 (value derived from Fig. 1 e) and zero otherwise; $P_{m/w}$ is the malting barley-to-wheat and $P_{m/f}$ the malting barley-to-fodder barley price ratio; P_w denotes the wheat price index. As the estimation results in Table 6 (upper part) show, the model fits the simulated results with R^2s around 0.9 for all scenarios and we can conclude that the model summarizes the simulation response well. The coefficients very clearly confirm the lower general malting barley supply

level and the steeper response curves to the malting-barley-to-wheat price ratios. They also show a flatter response curve with respect to wheat price levels and the malting barley-to-fodder price ratio.

To see how well the model generalizes, we constructed another LHS sample this time with 100 runs, in which no design point was exactly equal to any design point in the LHS600. We used the regression model estimated from the LHS600 to predict the malting barley supply at each design point of the LHS100 and compared them to the actual simulation results created by the MPMAS Central Swabian Jura for the LHS100. As a measure for goodness-of-fit, we calculated the Nash-Sutcliffe model efficiency with similar interpretation as the R^2. (In fact, for OLS regression they are equal.)

$$ME = 1 - \frac{\sum_i (Ypred_i - Yobs_i)^2}{\sum_i (Yobs_i - Yobs_{mean})^2} \qquad \text{(Eq. 3)}$$

As we can see from Table 6, goodness-of-fit for the validation sample is not very different from the R^2 for the LHS600 sample. We also reversed the experiment, estimating the regression model from the LHS100 and predicting simulation results for the LHS600 sample and obtained similar results with respect to goodness-of-fit (Tab. 6, lower part). There is some variation in the estimated coefficients providing an indication of the uncertainty introduced by sampling the design points. Still, differences between scenarios and orders of magnitudes of coefficients remain unaffected by this uncertainty.

4.5 Multivariate Adaptive Regression Splines and Kriging

We might be able to improve the fit of our regression model, e. g. including quadratic or cubic terms or more input factors or more interaction terms, but here we prefer to explore a different approach. Instead of defining a parametric regression model, as done step-by-step in the previous sections, we may also resort to a non-parametric, more automatized procedure in order to estimate a model that summarizes the simulation results of our agent-based model including potentially overlooked factor interactions. In the following, we use two non-parametric techniques, Multivariate Adaptive Regression Splines and Kriging.

The *Multivariate Adaptive Regression Splines* (Friedman 1991) technique automatically includes non-linearities and interactions between independent variables estimating a model of the form

$$f(x) = c_1 + \sum_{i=2}^{k} c_i B_i \quad \text{(Eq. 4)}$$

where B_i stands for a hinge function of the form $max(0, x-d)$ or $max(0, d-x)$, or a product of several such hinge functions (interactions between variables). The hinge functions allow for a continuous recursive partitioning of the input factor space that gives the approach its flexibility. The model is estimated in two passes. In a forward pass, the algorithm subsequently adds pairs of complementary hinge functions for a factor or factor interaction. It always chooses a partitioning for the factor or factor interaction that generates the strongest reduction in prediction error. This continues until an overall limit of terms is reached or a threshold of minimum improvement is not surpassed anymore. In the following backward pass, the algorithm prunes terms from the model in order to improve the generalizability of the model and reduce the danger of over-fitting. It prunes always the term that shows the least effectiveness with respect to a Generalized Cross Validation criterion.

We estimated four MARS models[3]: For the first (mars1), we allowed no interactions between variables; for the second (mars3), we allowed interactions up to the third degree; and for the third (mars10), up to the 10th degree. While for these first three model we allowed all 22 input factors to be included in the model trusting in the automatic selection capacity of the algorithm, the fourth MARS model (marsS) was restricted to consider only the four price coefficients ($prw_{mb}, prw_{fb}, prw_r, pc_w$) that showed a correlation with malting barley supply above 0.1 (cf. Section 4.2) with unrestricted interactions. Again, we estimated the models for the LHS600 sample and validated it against the LHS100 sample, and vice versa.

The formula for an estimated MARS model very easily gets large and is not necessarily easy to interpret. For space reasons, we report only the estimated formula for the mars1 model estimated for malting barley supply in scenario B from the LHS600 sample to provide an illustration what such a model may look like.

3 The MARS models were estimated using the R package DiceEval.

$$\begin{aligned}\hat{q}_{mb,s} = {} & 4{,}024 + 25{,}125\ max(0, prw_{mb} - 0.700) + 3024\ max(0, pc_w - 0.884) \\ & -16{,}022\ max(0, 0.884 - pc_w) + 59{,}810\ max(0, prw_{mb} - 0.875) \\ & -55{,}177\ max(0, prw_{mb} - 1.218) - 1{,}531\ max(0, 1.725 - pth) \\ & -5{,}383\ max(0, pc_{bf} - 0.930) - 4{,}775\ max(0, 0.920 - pc_{ft}) \\ & -2{,}454\ max(0, prw_r - 0.814) - 2{,}907\ max(0, 1.454 - man) \\ & -35{,}494\ max(0, prw_{fb} - 0.96)\end{aligned} \quad \text{(Eq. 5)}$$

Table 7 shows the model efficiencies for the different models for both samples. With the exception of the mars3 and mars10 models in scenario C2, all estimated models transfer well from the LHS600 to the LHS100 sample. When we censored model predictions, i. e. we corrected predictions of negative quantities to zero (shown in the fifth and eighth column), as one would certainly do when using the model to predict supply response, the deficiency in the fit of mars3 and mars10 is reduced. Notably, the model with preselected factors performs equally well as the automatic selection from the complete pool of factors. Generalization from the LHS100 to the LHS600 is considerably poorer, highlighting the danger of over-fitting incurred when using highly adaptive non-parametric methods.

Kriging originated as an interpolation method in geostatistics (Kleijnen 2009). Kriging predicts the value for an unobserved combination of independent variables – that means in our case a combination of input factors that has not been simulated – as a weighted combination of the observed (i. e. simulated) factor combinations. The weight for each observed factor combination is a function of the assumed correlation of its corresponding output with the output to be predicted as well as the assumed correlation of all other available factor combinations with the output to be predicted. This correlation is calculated based on the distance Δ between the observed and the new factor combination using a user-specified correlation function (here, we use a standard Gaussian correlation function $\rho = \prod_{j=0}^{k} \exp(-\theta \Delta_j^2)$). The weights (θ) reflect the importance of each input factor *j* in determining the distance and are estimated using maximum likelihood estimation (Kleijnen 2009).

Again, we estimated the model for the LHS600 sample and validated against the LHS100 sample, and vice versa. Table 8 shows the θ parameters estimated for each input factor. Generally, the higher θ, the lower the importance of the distance along this dimension of the input factor vector in determining the output. However, as our input factors are differently

scaled, we normalized each θ by the range of the associated input factor to translate them into a measure of importance of the input factor itself. Again, the three price coefficients (prw_{mb}, prw_{fb}, pc_w) stand out as clearly the most important determinants.

Model efficiencies for the Kriging models are listed in Table 8. The goodness-of-fit to the calibration sample is perfect by definition: The model simply reproduces the simulated output for an observed factor combination with a weight of 1, the weight for all other observed factor combinations is zero. As we can see from the table, the estimated Kriging model achieves the best fit when transferred from the LHS600 to the LHS100 sample. Performance for the generalization from LHS100 to LHS600 is again poorer, though still better than in the case of the MARS models.

5. Discussion

5.1 Simulated changes in supply response

Our simulation results suggest non-negligible changes to the regional malting barley, fodder barley and wheat supply under climate change. As anticipated, changes differ depending on assumed crop prices and as a consequence the supply functions do not merely experience a shift, but sensitivity to changes in price levels and price relations increases in some and decreases in other cases. Since we can expect prices to vary more often and rapidly than climate, this entails steeper, respectively flatter supply curves. The malting barley supply function is certainly the clearest example, for such a case. The two implemented adaptation scenarios show considerably different effects on supply functions, confirming the finding of Troost and Berger (2015) that it is important to take changes in crop rotation options and available days for field work into account when analyzing climate change adaptation in the area under study. In some cases, such as winter wheat supply, these non-yield effects exacerbate the effect of changes in crop yields, in others, such as summer fodder barley supply they reverse the simulated effect, and again in others, they exacerbate or reverse depending on the prevailing price environment. Which supply levels would finally be realized can, however, not be answered based on our agent-based model alone, since the simulated changes in supply and demand, together with developments in neighboring regions, would certainly trigger a price reaction of crop markets that is not captured

by our model. Here, we can only report on the simulated supply levels under all expected future price relations.

Our analysis also shows that the uncertain model parameters play only a minor role in determining the simulated malting barley supply response. Three to four price coefficients clearly dominate the estimated supply function. This is different, e. g in the case of wheat supply, which we did not analyze in more detail in this contribution. Here, three to five uncertain parameters play a non-negligible role in determining input supply. Though they do not affect the general direction of climate effects (Troost and Berger 2015), this needs to be taken into account when estimated functions are communicated. If such functions are then used to predict supply response, users will have to decide whether they choose uncertain parameter values consistent with their own assumptions or whether they treat the uncertainty as noise and average over function results of all parameter combinations (which would correspond to the multi-model average of an model ensemble).

5.2 Methods

Compared to the analysis of secondary data, simulation analysis has the advantage of being able to fully control for the influence of input factors on outcomes of interest. However, in reality, the computational burden and available time and resources limit the extent to which this potential for control can be realized. Full factorial designs for 22 input factors can hardly be realized with model run times of at least 20 minutes per run – especially, since a meaningful analysis of demand and supply functions usually requires assessing more than two levels, at least for the price coefficients.

Latin hypercube sampling is the experimental design of choice when it comes to obtaining the best global coverage of a factor space for a given, limited number of model runs. Since the value for a specific (continuous) input factor is unique to every design point of the LHS, however, result and sensitivity analysis must be restricted to methods that assume outcomes to be a locally smooth function of the input factors. A discrete methodology such as ANOVA, for example, would detect the common variation of all factors and would attribute all variance to a single factor or would require the analyst to classify the design points into meaningful groups.

The previous section illustrated how several such methods can be combined to explore and summarize the shifts in supply response predicted by an agent-based model. Each of the methods used has its strengths and weaknesses. Calculating a global mean and variance of the scenario differences over all design points provides a first overview and helps identifying those outcomes that show the most interesting developments. Analyzing correlations with input factors provides a starting point for disentangling the interrelationship between outcomes, price coefficients and uncertain model parameters. Scatter plots, scatter plot smoothers and regression analysis are certainly the methods that foster an understanding and communication of the mechanisms and interactions manifesting themselves in the simulation results.

By contrast, the output of the non-parametric methods can be more cryptic and much harder to communicate. For Kriging, for example, it is not enough to provide the estimated correlation functions, respectively θ, but also the design points and outcomes of the original model are required for prediction. Their strength is that they are able to automatically summarize the model behavior over the design space and predict model behavior at input factor combinations that have not been simulated. In this way, they can serve as surrogate models (or meta-models) for the actual simulation model that could e. g. be used for iterating with a national or global market model or estimated residual demand functions for the region in order to find a new equilibrium under climate change. Additionally, they may also help in the initial exploration and sensitivity analysis of the model results, highlighting which input factors might be worth considering in a regression model.

Our results for the MARS model remind us that flexible non-parametric methods always bear the danger of over-fitting, especially if the sample size is small. On the other hand, they may also help to design a simulation strategy to keep the number of evaluations of the original model low. For example, Kleijnen (2009) suggests to start by simulating the original model for a small initial sample, use Kriging to estimate a surrogate model, then generate a larger space-filling design and apply the surrogate model to it. Using a jackknife over the initial sample (or some other form of cross-validation), the uncertainty in the prediction of the surrogate model for each design point of the second sample can be estimated. One can then decide to simulate only the design points of the second sample that show the greatest uncertainty in order to improve the quality of the surrogate model with as few model runs as possible (Kleijnen 2009). Apart from MARS and

Kriging there are, of course, other nonparametric alternatives not tested in this analysis. Generalized Additive Models, for instance, provide a way to combine a parametric regression approach with nonparametric elements to capture nonlinearities.

6. Conclusions

The need to grow summer barley for rotational reasons is a good example for constraints to agricultural production that can be easily incorporated into a farm-level model, but are typically neglected in aggregate regional models or statistically estimated supply functions. Our results show that a potential change in the rotational compatibilities of crops under climate change may trigger non-negligible changes in aggregate supply functions for several crops. An agent-based model such as ours that explains aggregate regional supply bottom-up by disaggregating it to theoretically known (or empirically observable) processes (the agronomic and technical relationships determining the production conditions faced by farmers in the region) is able to derive conclusions about unobserved situations, such as climate change, that may entail structural breaks in the underlying interdependencies.

We estimated the supply functions based on a space-filling experimental design that allows to globally cover all combinations of anticipated price relations as well as considering the uncertainty in the simulation model. The mutual interactions between variables observed in our results underline that a simple, one-factor-at-a-time (*ceteris paribus*) variation of input factors would only provide a very incomplete picture of the simulated supply response behavior, in comparison.[4]

We employed a range of different statistical methods to explore and describe the supply response curves entailed by the results of our simulation experiments. Besides, standard regression analysis, we use Multivariate Adaptive Regression Splines and Kriging to summarize the model response and interpolate outcomes for input factor combinations that had not been simulated. Kriging showed a better performance in our example, but is also computationally more costly in estimation and prediction.

4 On the inadequacy of one-at-a-time sensitivity analysis, cf. also Saltelli and Annoni (2010).

Both, regression models and non-parametric models may serve as surrogate models for the agent-based model in order to interpolate model outcomes that have not been simulated in situations where many different model solutions are required and solving the original model is too costly. This could for example be used to iterate a farm-level model, respectively its surrogate, with a global or partial equilibrium model (or alternatively estimated residual demand functions). In this way, feedbacks from agricultural markets could be considered in the agent-based model and the equilibrium model could profit from the updated regional supply functions. Certainly important questions remain to be discussed in this context, but we think that such an endeavor could be worthwhile to pursue and would allow the different classes of models to better complement each other in the context of climate change adaptation and policy analysis (Troost and Berger 2015).

Here, we advanced a step into this direction by demonstrating the feasibility of using a regionalized farm-level models for a process-based simulation of regional agricultural supply functions. Although we used a non-connected agent-based model without interactions and abstracted from the time dimension by simulating only one period under different scenarios, the approach is directly applicable to fully connected agent-based models that take interactions (e. g. land markets, innovation diffusion, inter-farm cooperation, farm succession) into account and are run over multiple periods allowing a recursive-dynamic simulation of structural change in agriculture.

References

Antle, J. M., Capalbo, S. M., 2001**,** Econometric-Process Models for Integrated Assessment of Agricultural Production Systems. Am. J. Agr. Econ. 83, 389-401.

Aurbacher, J., Parker, P. S., Calberto Sánchez, G. A., Steinbach, J., Reinmuth, E., Ingwersen, J., Dabbert, S., 2013, Influence of climate change on short term management of field crops – A modelling approach. Agr. Syst. 119, 44-57.

Berendonk, C., 2011, Standortgerechte Weide- und Mähweidenutzung des Dauergrünlands - Grünlandanlage, Pflege, Düngung, Nutzung, Weidemanagement. Landwirtschaftskammer Nordrhein-Westfalen, Kleve.

Berger, T., Schreinemachers, P., Woelcke, J., 2006, Multi-agent simulation for the targeting of development policies in less-favored areas. Agr. Syst. 88, 28-43.

Berger, T. , Troost, C., 2014, Agent-based Modelling of Climate Adaptation and Mitigation Options in Agriculture, J. Agr. Econ., 65, 323-348.

Buysse, J., Huylenbroeck, G. V., Lauwers, L., 2007, Normative, positive and econometric mathematical programming as tools for incorporation of multifunctionality in agricultural policy modelling, Agr. Ecosyst. Environ. 120, 70-81.

Campolongo, F., Cariboni, J., Saltelli, A., 2007, An effective screening design for sensitivity analysis of large models. Environ. Modell. Softw. 22, 1509-1518.

destatis, 2011, Arbeitskräfte - Landwirtschaftszählung 2010. Land- und Forstwirtschaft, Fischerei, Fachserie 3, Heft 2, Statistisches Bundesamt, Wiesbaden.

destatis, 2012a, GENESIS online - Tabelle 12411-0008: Bevölkerung Deutschland. https://www.genesis.destatis.de/genesis/on line/data?operation=abruftabellenVerzei chnis

destatis, 2012b, GENESIS online - Tabelle 12612-0008: Geburtenziffern Deutschland. https://www.genesis.destatis.de/genesis/on line/data?operation=abruftabellenVerzei chnis

destatis, 2012c, GENESIS online - Tabelle 12613-0003: Gestorbene Deutschland. https://www.genesis.destatis.de/genesis/on line/data?operation=abruftabellenVerzei chnis

destatis, 2012d, GENESIS online - Tabelle 61221-0002: Index der Einkaufspreise landwirtschaftl. Betriebsmittel: Deutschland, Wirtschaftsjahr, Messzahlen mit/ohne Umsatzsteuer, Landwirtschaftliche Betriebsmittel. https://www.genesis.destatis.de/genesis/on line/data?operation=abruftabellenVerzei chnis

Forschungsdatenzentrum der Statistischen Ämter des Bundes und der Länder [FDZ], 2010, AFiD-Panel Agrarstruktur 1999, 2003, 2007. Fors chungsdatenzentrum der Statistischen Ämter des Bundes und der Länder, Düsseldorf/Kiel.

Friedman, J. H., 1991, Multivariate adaptive regression splines. The Annals of Statistics 19, 1-67.

Gibbons, J., Wood, A., Craigon, J., Ramsden, S., Crout, N., 2010, Semi-automatic reduction and upscaling of large models: A farm management example, Ecol. Model. 221, 590 – 598.

Jakeman, A., Letcher, R., Norton, J., 2006, Ten iterative steps in development and evaluation of environmental models. Environ. Modell. & Softw. 21, 602-614.

Kleijnen, J. P., 2009, Kriging metamodeling in simulation: A review. Eur. J. Oper. Res. 192, 707-716.

Kuratorium für Technik und Bauwesen in der Landwirtschaft e.V [KTBL], 2010, KTBL-Datensammlung. Betriebsplanung Landwirtschaft 2010/11. Kuratorium für Technik und Bauwesen in der Landwirtschaft e.V., Darmstadt.

Landesanstalt für Entwicklung der Landwirtschaft und der ländlichen Räume [LEL], 2010, Material aus der Ernährungswirtschaft des Landes Baden-Württemberg: Getreide und Futtermittel 2008/2009. Landesanstalt für Entwicklung der Landwirtschaft und der ländlichen Räume, Schwäbisch Gmünd.

Landesanstalt für Entwicklung der Landwirtschaft und der ländlichen Räume [LEL], 2011a, Material aus der Ernährungswirtschaft des Landes Baden- Württemberg: Milch 2010. Landesanstalt für Entwicklung der Landwirtschaft und der ländlichen Räume, Schwäbisch Gmünd.

Landesanstalt für Entwicklung der Landwirtschaft und der ländlichen Räume [LEL], 2011b. Material aus der Ernährungswirtschaft des Landes Baden- Württemberg: Vieh und Fleisch 2010. Landesanstalt für Entwicklung der Landwirtschaft und der ländlichen Räume, Schwäbisch Gmünd.

LfL (Ed.), 2010, Gruber Tabelle zur Füutterung der Milchkühe Zuchtrinder Schafe Ziegen, 32nd Edition. Bayerische Landesanstalt für Landwirtschaft, Freising-Weihenstephan.

LfL (Ed.), 2011, Gruber Tabelle zur Fütterung in der Rindermast: Fresser, Bullen, Ochsen, Mastfärsen, Mastkühe, 16th Edition. Bayerische Landesanstalt für Landwirtschaft, Freising-Weihenstephan.

McKay, M. D., Beckman, R. J., Conover, W. J., 1979, A Comparison of Three Methods for Selecting Values of Input Variables in the Analysis of Output from a Computer Code. Technometrics 21, 239-245.

Reidsma, P., Ewert, F., Lansink, A. O., Leemans, R., 2010, Adaptation to climate change and climate variability in European agriculture: The importance of farm level responses. Eur. J. Agron., 32, 91-102.

Rizzo, M. L., Szekely, G., 2013, energy : E-statistics (energy statistics). R package version 1.6.

Saltelli, A., Tarantola, S., Campolongo, F., Ratto, M., 2004, Sensitivity analysis in practice. - A guide to assessing scientific models. Wiley, Chichester, UK.

Saltelli, A., Annoni, P., 2010, How to avoid a perfunctory sensitivity analysis. Environ. Modell. Softw. 25, 1508-1517.

Schreinemachers, P., Berger, T., 2011**,** MP-MAS: An agent-based simulation model of human-environment interaction in agricultural systems. Environ. Modell. Softw. 26, 845-859.

Szekely, G., Rizzo, M. L., Bakirov, N. K., 2007, Measuring and testing dependence by correlation of distances. Ann. Stat. 35, 2769-2794.

Szekely, G. J., Rizzo, M. L., 2013, Energy statistics: A class of statistics based on distances. J. Stat. Plan. Infer. 143, 1249-1272.

Troost, C., Calberto, G., Berger, T., Ingwersen, J., Priesack, E., Warrach-Sagi, K. and Walter, T. , 2012, Agent-based modeling of agricultural adaptation to climate change in a mountainous area of South West Germany, in R. Seppelt, A. Voinov, S. Lange and D. Bankamp, eds., International Environmental Modelling and Software Society (iEMSs): 2012 International Congress on Environmental Modelling and Software Managing Resources of a Limited Planet, Sixth Biennial Meeting, Leipzig, Germany. http://www.iemss.org/society/index.php/iemss-2012-proceedings

Troost, C., 2014, MPMAS Central Swabian Jura (Version 3.1) - Model Documentation, University of Hohenheim, Stuttgart. https://mp-mas.uni-hohenheim.de/documentation

Troost, C., Berger, T., 2015, Dealing with Uncertainty in Agent-Based Simulation: Farm-Level Modeling of Adaptation to Climate Change in Southwest Germany, Am J. Agr. Econ. 97: 833-854.

van Wijk, M., Rufino, M., Enahoro, D., Parsons, D., Silvestri, S., Valdivia, R., Herrero, M., 2012, A review on farm household modelling with a focus on climate change adaptation and mitigation. CGIAR Research Program on Climate Change, Agriculture and Food Security (CCAFS), CCARFS Working Paper No. 20, Kopenhagen.

Tables and Figures

Table 1. Compatibility of Crops in Rotation (Troost & Berger, ibid.)

	Following crop						
Preceding crop	FA	FG	SM	SB	WB	WR	WW
Fallow	1	1	1	1	1	1	1
Field grass	1/2	2/3	1/2	1/2	1/2	0	1/2
Silage maize	1	1	X	1	0	0	1
Summer barley	1	1	1	1/2	1	1	0
Winter barley	1	1	1	1	0	1	0
Winter rapeseed	1	1	1	1	1	0	1
Winter wheat	1	1	1	1	0	CC	1/2

Note:
0: incompatible
1: compatible, full area can be considered for following crop
1/2: maximum half of the area can be considered, e. g. wheat can directly follow wheat only once, then another crop has to be grown before wheat can be grown again
2/3: Field grass is a semi-permanent culture that is usually kept 2-3 years on the same field. So at maximum half the area can be considered preceding crop for other crops and at maximum 2/3 can be considered preceding crop for next year's fields grass.
X: uncertain, subject to calibration
CC: 0 in the baseline, 1 if climate change shifts crop management dates

Table 2. Price coefficients used for price variation in the experimental design

Item	Symbol	Range	Avg. ratio
Beef & young cattle	pc_{bf}	[0.7, 1.3]	
Fertilizer	pc_{ft}	[0.5, 2]	
Fuel & energy	pc_{fu}	[0.7, 1.5]	
Milk	pc_{mi}	[0.7, 1.2]	
Pork & pigs	pc_{pk}	[0.7, 1.3]	
Wheat	pc_{w}	[0.5, 2]	
Animal feed (rel. to wheat price development)	prw_{af}	[0.7, 1.5]	var.
Grain maize (rel. to wheat price development)	prw_{mg}	[0.8, 1.2]	1.02
Malting barley (rel. to wheat price development)	prw_{mb}	[0.7, 1.3]	1.175
Fodder barley (rel. to wheat price development)	prw_{fb}	[0.9, 1.2]	0.908
Rapeseed (rel. to wheat price development)	prw_{r}	[0.7, 1.4]	2.032

Table 3. Unfixed parameters representing uncertainty in the MPMAS Central Swabian Jura model (own compilation based on Troost & Berger, ibid.)

fgl	Scaling parameter for the amount of labor required for fresh grass harvest
chp	Demand for excess heat of biogas electricity production (yes/no)
man	Scales the maximum manure application
bbp	Supply of brewery byproducts for feeding (yes/no)
bfp	Birth factor in the past (affects current household size)
clr	KTBL climatic region for time slots of field work.
scm	Probability that a male child is interested in taking over the farm
pth	Probability to be able to hire a machinery service provider per day with suitable weather.
ywh	Scaling parameter for the maximum wheat yield
wfh	Scaling parameter for the price for hiring machinery services
pop	Chosen starting population

Table 4. Overview of average climate effects on supply and demand of selected crops and its variation over the experimental design.

	B	C1		C2	
Simulated outcome	RSDb	Md1/Mb	RSDd1	Md2/Mb	RSDd2
Malting barley sales [t]	0.94	0.18	1.17	-0.02	20.19
Fodder barley sales [t]	0.62	-0.25	0.65	-0.53	0.49
Fodder barley purchases [t]	1.04	0.04	2.06	0.07	3.08
Wheat sales [t]	0.27	0.22	0.30	0.49	0.29
Wheat purchases [t]	2.02	-0.18	2.09	-0.36	2.07

Table 5. Distance correlations between supply of/demand for selected crops with selected price coefficients and uncertain model parameters.

		Malting barley sales	Fodder barley sales	Fodder barley purchases	Wheat sales	Wheat purchases
Scenario B	prw_{af}	0.05	0.06	0.16	0.13	0.09
	prw_{mg}	0.09	0.08	0.35	0.22	0.33
	prw_{mb}	0.87	0.53	0.14	0.25	0.04
	prw_{fb}	0.21	0.65	0.68	0.57	0.41
	prw_{r}	0.08	0.07	0.07	0.10	0.06
	pc_{w}	0.18	0.21	0.15	0.30	0.11
	pc_{pk}	0.06	0.09	0.14	0.05	0.06
	bbp	0.05	0.05	0.18	0.21	0.43
	clr	0.02	0.09	0.03	0.14	0.03
	pth	0.07	0.17	0.06	0.31	0.09
	ywh	0.05	0.06	0.06	0.18	0.04
	wfh	0.05	0.07	0.06	0.10	0.11
Scenario C1	prw_{af}	0.05	0.07	0.16	0.14	0.09
	prw_{mg}	0.08	0.09	0.34	0.20	0.33
	prw_{mb}	0.88	0.60	0.15	0.31	0.04
	prw_{fb}	0.20	0.53	0.68	0.45	0.40
	prw_{r}	0.09	0.09	0.08	0.12	0.06
	pc_{w}	0.19	0.22	0.16	0.24	0.10
	pc_{pk}	0.06	0.09	0.14	0.05	0.06
	bbp	0.06	0.06	0.17	0.23	0.43
	clr	0.03	0.10	0.03	0.17	0.04
	pth	0.08	0.24	0.06	0.41	0.11
	ywh	0.06	0.06	0.05	0.18	0.04
	wfh	0.05	0.07	0.06	0.08	0.12
Scenario C2	prw_{af}	0.04	0.06	0.13	0.09	0.07
	prw_{mg}	0.08	0.06	0.37	0.18	0.34
	prw_{mb}	0.92	0.54	0.09	0.49	0.05
	prw_{fb}	0.16	0.57	0.68	0.42	0.39
	prw_{r}	0.11	0.05	0.07	0.07	0.06
	pc_{w}	0.14	0.35	0.20	0.34	0.13
	pc_{pk}	0.06	0.08	0.13	0.05	0.06
	bbp	0.05	0.05	0.18	0.18	0.42
	clr	0.02	0.04	0.04	0.04	0.03
	pth	0.06	0.14	0.04	0.21	0.09
	ywh	0.08	0.08	0.06	0.20	0.04

wfh	0.05	0.06	0.06	0.09	0.11

Table 6. OLS regression of malting barley supply on selected price relations.

		B		C1		C2	
Sample	var	coeff	se	coeff	se	coeff	se
LHS600	*Constant*	29	296	135	332	49	288
	D	-67,943	2,008 ***	-69,991	2,252 ***	-89,599	1,951 ***
	D * P_m/w	38,370	2,260 ***	45,817	2,535 ***	63,564	2,196 ***
	D * P_m/f	22,120	1,887 ***	18,282	2,117 ***	16,377	1,833 ***
	D * P_w	8,053	486 ***	9,273	545 ***	5,483	472 ***
	R^2	0.906		0.908		0.923	
	ME LHS100	0.904		0.885		0.922	
LHS100	*Constant*	140	758	599	938	379	824
	D	-69,606	5,013 ***	-69,519	6,201 ***	-91,863	5,449 ***
	D * P_m/w	39,267	5,820 ***	40,210	7,198 ***	66,611	6,326 ***
	D * P_m/f	21,663	5,098 ***	23,011	6,305 ***	16,862	5,541 ***
	D * P_w	9,244	1,251 ***	9,593	1,547 ***	3,691	1,359 ***
	R^2	0.905		0.886		0.905	
	ME LHS600	0.904		0.906		0.919	

Table 7. Goodness-of-fit of Estimated MARS and Kriging Models for Malting Barley Supply.

		Goodness-of-fit					
		Estimated from LHS600			Estimated from LHS100		
Scenario	Model	LHS600	LHS100	LHS100 (cens)	LHS100	LHS600	LHS600 (cens)
B	MARS (no int.)	0.889	0.865	0.881	0.878	0.872	0.882
	MARS (3-way int.)	0.934	0.899	0.906	0.938	0.747	0.762
	MARS (10-way int.)	0.933	0.914	0.921	0.950	0.836	0.849
	MARS (preselected)	0.918	0.907	0.914	0.924	0.860	0.869
	Kriging	1.000	0.955	0.956	1.000	0.851	0.854
C1	MARS (no int.)	0.895	0.869	0.883	0.964	0.852	0.872
	MARS (3-way int.)	0.946	0.903	0.911	0.987	0.703	0.713
	MARS (10-way int.)	0.946	0.903	0.911	0.948	0.783	0.811
	MARS (preselected)	0.924	0.910	0.920	0.924	0.759	0.796
	Kriging	1.000	0.976	0.976	1.000	0.921	0.924
C2	MARS (no int.)	0.942	0.936	0.943	0.920	0.766	0.783

MARS (3-way int.)	0.973	-0.356	0.910	0.952	0.754	0.784
MARS (10-way int.)	0.973	-0.453	0.771	0.987	0.703	0.713
MARS (preselected)	0.958	0.946	0.948	0.969	0.854	0.856
Kriging	1.000	0.959	0.959	1.000	0.906	0.914

Table 8. Estimated Thetas for Input Factors for the Kriging Model of Malting Barley Supply.

	B		C1		C2	
Parameter	Theta	nTheta	Theta	nTheta	Theta	nTheta
pc_{bf}	2.81	4.68	2.19	3.65	2.42	4.04
pc_{ft}	8.71	5.82	11.21	7.49	6.01	4.02
pc_{fu}	4.44	5.56	7.99	10.00	7.99	10.00
pc_{mk}	3.10	6.20	4.03	8.07	4.99	10.00
pc_{pk}	1.58	2.63	1.57	2.61	1.58	2.63
pc_{w}	0.45	0.30	0.42	0.28	0.71	0.47
prw_{af}	1.59	1.99	5.43	6.79	3.40	4.26
prw_{mg}	3.56	8.93	3.99	10.00	3.99	10.00
prw_{mb}	0.06	0.10	0.06	0.10	0.07	0.12
prw_{fb}	0.08	0.26	0.11	0.37	0.18	0.60
prw_{r}	1.55	2.22	1.50	2.15	0.79	1.12
fgl	12.96	6.50	6.70	3.36	19.95	10.00
chp	10.00	10.00	10.00	10.00	2.75	2.75
man	1.73	3.46	1.89	3.79	0.48	0.96
bbp	8.14	8.14	7.16	7.16	10.00	10.00
bfp	0.50	10.00	0.42	8.50	0.14	2.81
clr	7.62	7.62	10.00	10.00	10.00	10.00
scm	4.54	9.08	5.00	10.00	5.00	10.00
pth	1.79	1.20	1.60	1.07	2.48	1.65
ywh	0.16	1.67	0.28	2.88	0.18	1.87
wfh	5.48	5.65	9.08	9.36	8.83	9.11
pop	11.36	5.68	8.77	4.38	13.92	6.96
trend	13,923		16,362		16,731	

Note:
nTheta: Theta normalized by the range of the input factor.

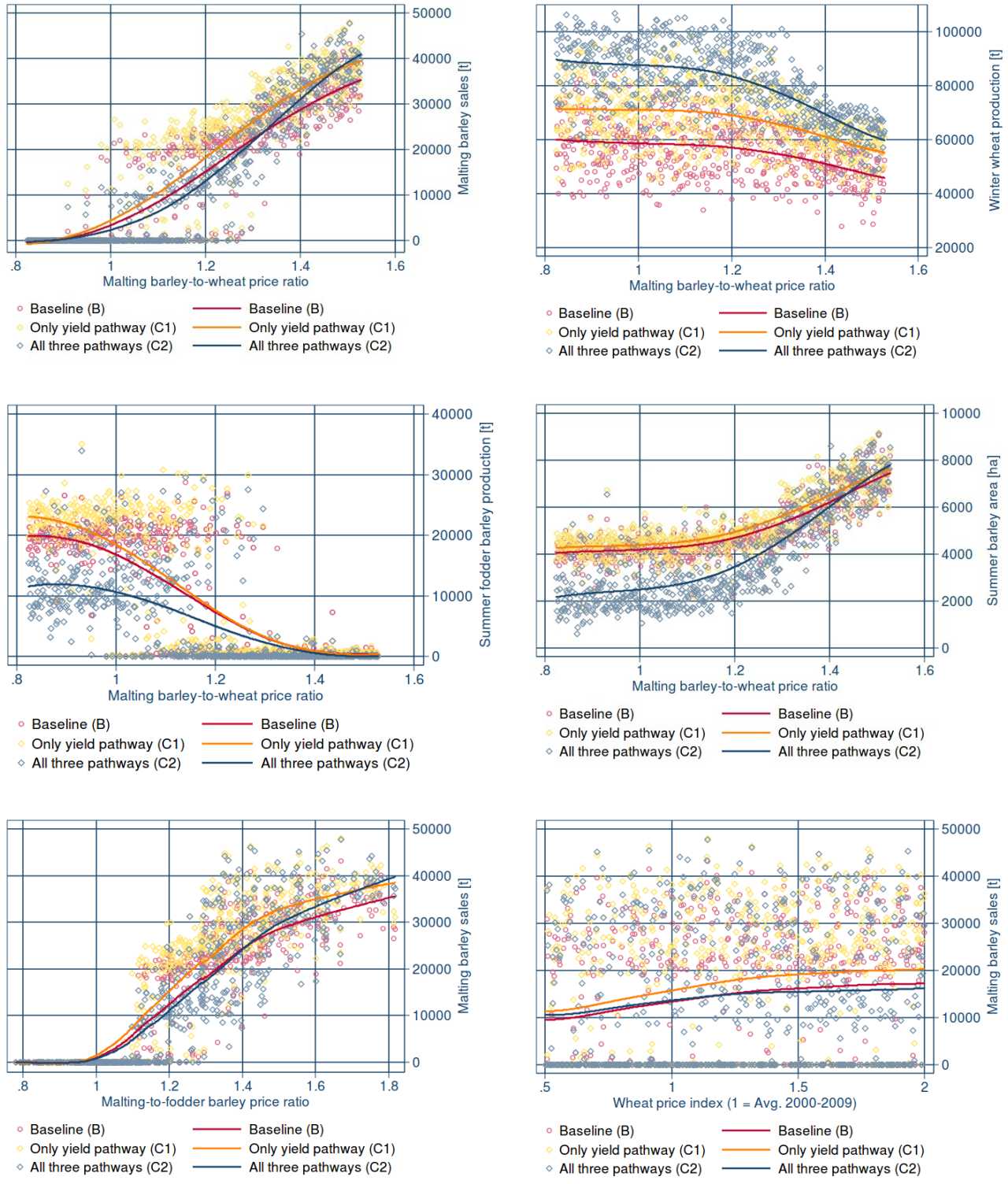

Figure 1: Scatterplots with overlaid LOWESS smoothers relating barley and wheat supply to selected price ratios for the three scenarios: (a) malting barley sales, (b) winter wheat production, (c) summer fodder barley production, and (d) summer barley area related to the malting barley-to-wheat price ratio as well as malting barley sales related to (e) the malting-to-fodder barley price ratio and the (f) wheat price index

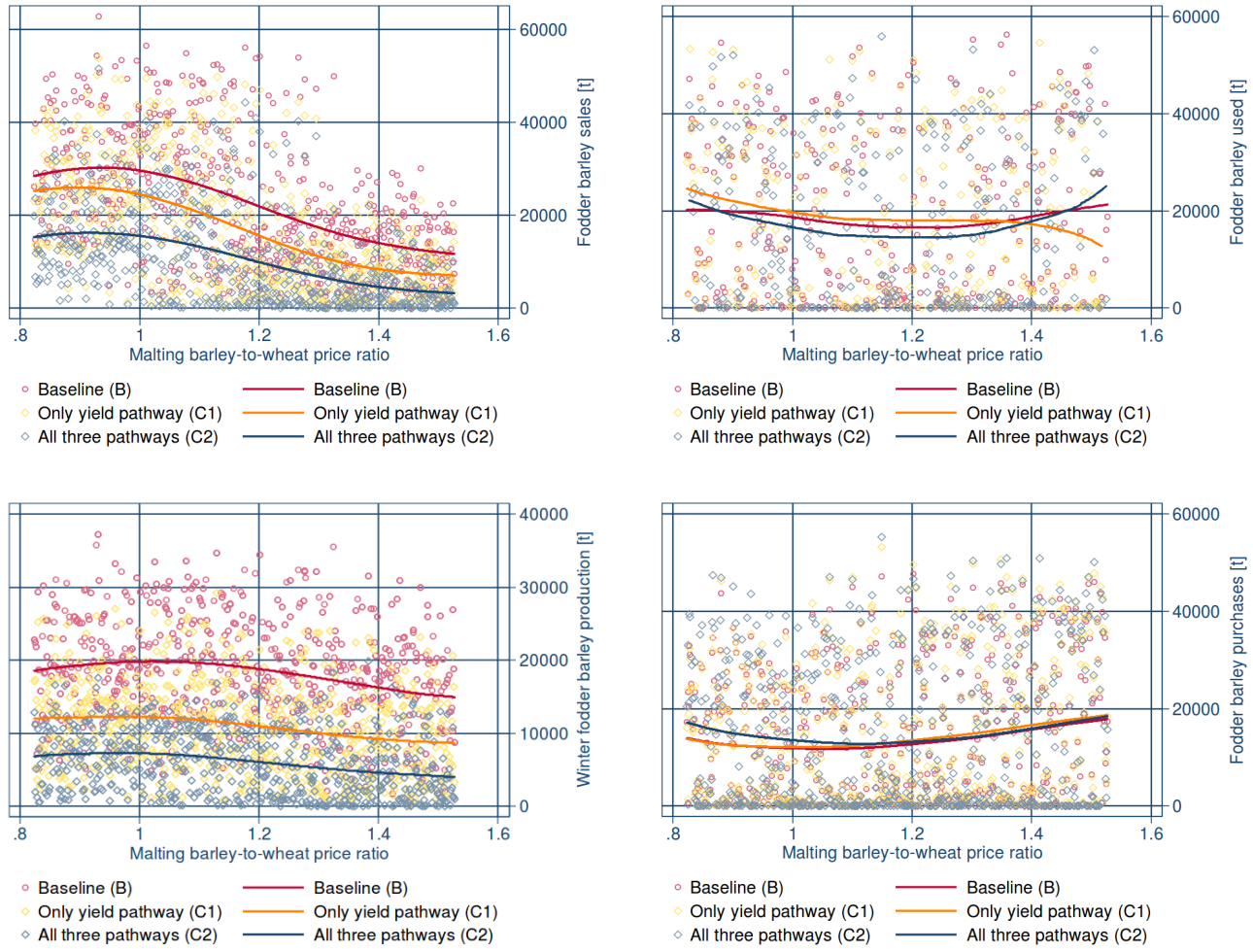

Figure 2. Scatter plots with overlaid LOWESS smoothers depicting the relationship of (a) fodder barley sales, (b) fodder barley use for feeding, (c) winter fodder barley production and (d) fodder barley purchases to the malting barley-to-wheat price ratio in the three scenarios.